Article

Insights into the Genes Involved in ABA Biosynthesis and Perception during Development and Ripening of the Chilean Strawberry Fruit

María A. Moya-León [1*], Yazmina Stappung [1], Elena Mattus-Araya [1] and Raúl Herrera [1]

[1] Laboratorio de Fisiología Vegetal y Genética Molecular, Instituto de Ciencias Biológicas, Universidad de Talca, 3465548 Talca, Chile; alemoya@utalca.cl (M.A.M.-L.); ystappung@utalca.cl (Y.S.); elena.mattus@utalca.cl (E.M.-A.); raherre@utalca.cl (R.H.)

* Correspondence: alemoya@utalca.cl.

Abstract: Hormones act as master ripening regulators. In non-climacteric fruit ABA plays a key role in ripening. Recently we confirmed in *Fragaria chiloensis* fruit that in response to ABA treatment the fruit induces ripening associated changes such as softening and color development. In consequence with these phenotypic changes, transcriptional variations associated with cell wall disassembly and anthocyanins biosynthesis were reported. As ABA stimulates ripening of *F. chiloensis* fruit, the molecular network involved in ABA metabolism was analyzed. Therefore, the expression level of genes involved in ABA biosynthesis and ABA perception were quantified during development of the fruit. Four *NCED/CCDs* and 6 *PYR/PYLs* family members were identified in *F. chiloensis*. Bioinformatics analyses confirmed the existence of key domains related to functional properties. Through RT-qPCR analyses the level of transcripts were quantified. *FcNCED1* codifies a protein that displays crucial functional domains and the level of transcripts increased as the fruit develops and ripens, in parallel with the increment in ABA. In addition, *FcPYL4* codifies for a functional ABA receptor and its expression follows an incremental pattern during ripening. The study concludes that *FcNCED1* is involved in ABA biosynthesis, meanwhile *FcPYL4* participates in ABA perception during ripening of *F. chiloensis* fruit.

Keywords: ABA biosynthesis; ABA perception; *Fragaria chiloensis*; fruit ripening; NCED; PYR/PYL receptors; phylogenic analysis; RT-qPCR

1. Introduction

Chilean strawberry (*Fragaria chiloensis*) is a native wild species from Chile that produces a fruit which is highly appreciated for its good organoleptic qualities such as aroma and taste, its exotic white color and remarkable biotic stress tolerance [1-3]. Albeit those extraordinary properties, the fruit softens very fast and intensively during ripening that reduces its postharvest shelf-life.

The Chilean strawberry fruit ripens with a non-climacteric pattern. Ripening is a complex process, during which a fruit develops into a fleshy, colorful and tasty fruit. For these biochemical and physiological changes a series of metabolic pathways are switched on, such as degradation of chlorophyll and starch, biosynthesis of pigments and volatile compounds, accumulation of sugars and organic acids [4]. It is important to highlight that the perfect coordination of those metabolic pathways is needed to develop a fruit of good quality. In climacteric fruits most of those metabolic pathways are regulated and coordinated by the hormone ethylene, however in non-climacteric fruit ethylene does not have the same effect [5]. Several hormones have been analyzed as master ripening regulators in non-climacteric fruit, including abscisic acid (ABA) and auxins.

Hormones play essential roles in the control and coordination of several physiological events, including fruit ripening. In strawberry, hormonal changes include the rise of ABA levels along the ripening development, and this increment coincides with the drop of auxins [6]. Several reports have shown that ABA promotes the ripening of strawberry fruit. It has been documented in different species of *Fragaria* that the treatment of turning or ripe strawberry fruits with ABA promotes a full ripe phenotype [7-11]. Treatments of fruit with ABA at the green stage and still attached to the plant, also promotes ripening [12]. On the other hand, auxins seem to delay ripening of non-climacteric fruit. This has been proven by the exogenous application of auxins that delays ripening development

 doi:10.20944/preprints202304.0574.v1

of strawberry fruit, and by the removal of the endogenous source of auxins (the achenes) that promotes the ripening of *F. x ananassa* fruit [13]. Recently, it has been shown in *F. vesca* that even if auxins levels are relatively low and stable in advanced ripening fruit stages, the expression of genes related to auxin signal transduction and down-stream responses are reduced in receptacles as ABA increases [14]. Therefore, although the ABA/auxins ratio has been proposed as the coordination of fruit development and ripening in strawberry fruit [5,9], new evidences suggest that ABA could be the master regulator hormone and a key controller of gene expression during strawberry ripening [10,11].

ABA is a sesquiterpenoid hormone synthesized through the carotenoid pathway, also known as the 'indirect pathway' [15]. This pathway, widely reviewed by [16,17], initiates in plasmids with the conversion of zeaxanthin into trans-violaxanthin, a C40 precursor, by zeaxanthin epoxidase (ZEP); at this point the pathway diverges in two ways, leading to the conversion of 9'-cis-neoxanthin or 9'-cis-violaxanthin, which are then converted into xanthoxin (C15 intermediate) through an oxidative cleavage by the 9-cis-epoxycarotenoid dioxygenase (NCED); then an alcohol dehydrogenase at cytosol converts xanthoxin into abscisic aldehyde; finally the abscisic aldehyde is oxidized to ABA by an abscisic aldehyde oxidase (AAO). On the other hand, ABA catabolism is mediated by CYP707A, a cytochrome P450 monooxygenase that converts ABA into phaseic acid (PA) through a catalytic hydroxylation [18]. The second form of catabolism is the conjugation of ABA by a UDP-glucosyltransferase (UGT) to form ABA-glucose ester (ABA-GE), which is an inactive form of ABA that is stored in vacuoles and the endoplasmic reticulum [19,20]. ABA-GE can be reversibly transformed into ABA by β-glucosidases and released from the endoplasmic reticulum and vacuole [21]. Therefore, ABA levels in the fruit are controlled through the balance between its biosynthesis (*NCED*) and its catabolism (*CYP707A*) [22].

ABA cellular responses are mediated by a group of soluble proteins named pyrabactin resistant (PYR) and PYR-like (PYL) receptors (reviewed by [15]). The activation of these receptors by ABA induces the formation of a complex with the protein phosphatase 2C (PP2C), and in consequence PP2C releases SNF1-related kinases (SnRK). Then SnRK can phosphorylate targets such as transcription factors, ion channels, Raf-like MAPKKKs signaling pathway and other mediators of ABA response (reviewed by [23]). It has been described that PYLs such as AtPYL4-6 and AtPYL8-10 act as monomers and have higher ABA binding affinity, interacting with PP2Cs in an ABA-enhanced manner; meanwhile PYLs such as AtPYR1 and AtPYL1-2 act as dimers and have lower ABA binding affinity, interacting with PP2Cs in an ABA-dependent manner [24].

ABA homeostasis and ABA perception have been mainly investigated in *F. x ananassa* and *F. vesca.* The key role of NCED on ABA biosynthesis in strawberry fruit was demonstrated on transgenic *FaNCED1* RNAi fruit [12] that provides transgenic fruit with reduced ABA levels compared to control fruit. In addition, the fruit remains uncolored, however the exogenous application of ABA recovered the normal red color of the fruit. During development of strawberry fruit, the expression of *FaNCED1* and *FaNCED2* rises as the levels of ABA levels increases, meanwhile the expression of *FaCYP707A1* increases from green to white fruit, then decreases until the final stages of ripening [25]. On the other hand, nine members of the *FaPYR/PYL* gene family have been identified in *F. x ananassa*, and reports indicate that *FaPYL2* may play a major role in ripening [26]. In *F. vesca* ABA homoeostasis involves the regulation of ABA catabolism and biosynthesis by feedback and feedforward loops which are linked to the repression of *CYP707A* expression and promotion of *NCED* expression at the onset of ripening [27]. In addition, the transient silencing of *FveCYP707A4a*, that increases the expression of *FveNCED5* and rises the levels of ABA, induces the expression of genes related to fruit softening (*FvePL*) [27]. *FvePYL2* transcripts reached a relatively high expression level at the red fruit stage, while other *FvePYLs* have diversified expression patterns [14].

In *F. chiloensis* several evidences confirm that ABA is involved in its ripening as it can induces the transcriptional changes required for fruit softening and color development [5,10,11,28-30]. As ABA seems to have a key participation in ripening stimulation of *F. chiloensis* fruit, the molecular network involved in ABA metabolism in ripening fruit was analyzed. Currently, there are some evidences of the participation of *NCEDs* on *F. chiloensis* fruit [11], but none for *PYR/PYLs*. Therefore,

Preprints (www.preprints.org) | NOT PEER-REVIEWED | Posted: 19 April 2023 doi:10.20944/preprints202304.0574.v1

the expression level of genes involved in ABA biosynthesis and ABA perception were quantified in *F. chiloensis* fruit as a way to provide further molecular evidences of the participation of ABA on the ripening development of this fruit. As several *NCEDs* and *PYR/PYLs* family members have been identified in fruit species but only few of them seems to participate during fruit ripening, this work pretends to identify those members involved in the ripening of this non-climacteric fruit.

2. Results

2.1. Identification of FcNCED/CCDs family genes and analysis of deduced amino acid sequences

Through the annotation process by different databases, it was possible to identify two *NCEDs* and two *CCDs* sequences (*FcNCED1*, *FcNCED3*, *FcCCD1* and *FcCCD4*) into the *F. chiloensis* transcriptome (Table 1). These sequences were named according to their closest relative sequence within the *F. vesca* genome.

Table 1. Analysis of functional domains of deduced FcNCED/CCD amino acid sequences using PFAM database.

Gene	Transcript ID	Domain type	Seq length (aa)
FcNCED1	comp919_c0_seq1	Retinal pigment epithelial membrane protein	501
FcNCED3	comp27198_c0_seq1	Retinal pigment epithelial membrane protein	392
FcCCD1	comp799_c0_seq1	Retinal pigment epithelial membrane protein	568
FcCCD4	comp503_c0_seq1	Retinal pigment epithelial membrane protein	581

The analysis of their coding sequences recognized the characteristic domain of NCED/CCD proteins 'Retinal pigment epithelial membrane protein' (RPE65) in all sequences, domain responsible for the binding of Fe^{2+}. An evolutionary relationship study between different rosaceas species (*F. x ananassa, F. vesca, M. domestica, R. chinensis, R. rugosa* and *P. avium*), *A. thaliana* and *F. chiloensis* provided a phylogenetic tree that clearly separates NCEDs from CCDs into different subfamilies, and CCD comprises two clades (CCD1 and CCD4) (Figure 1). The translated amino acid sequences of *F. chiloensis* share high sequence identity with *F. vesca* and *F. x ananassa*, confirming the parental relationship with this last species.

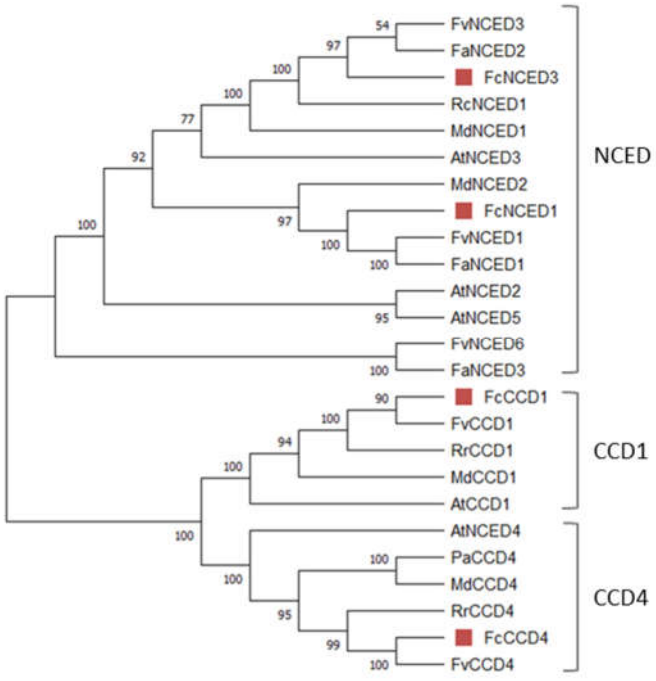

Figure 1. Phylogenetic analysis of FcNCEDs and FcCCDs proteins. Different *F. chiloensis* sequences (4) were aligned with 21 sequences from *F. x ananassa* (3), *M. domestica* (4), *R. chinensis* (1), *R. rugosa* (2), *P. avium* (1), *F. vesca* (5) and *A. thaliana* (5). The phylogenic tree was built using the Neighbor-

Preprints (www.preprints.org) | NOT PEER-REVIEWED | Posted: 19 April 2023 doi:10.20944/preprints202304.0574.v1

Joining method with bootstrap consensus tree inferred from 5000 replicates. The list of protein sequences employed in the analysis, including Genbank accession numbers, is shown in Table S1.

A comparative alignment was performed between the deduced protein sequences of *FcNCEDs* and *FcCCDs* and that of the crystal ZmVP14 (maize viviparous14, a key enzyme in the biosynthesis of ABA) (PDB code: 3NPE) (Figure 2) [31]. The alignment showed that the sequences share cleavage domain 2 (CV2) that interacts with 9 cis-violaxanthin, and partly CV1 (Figure 2, green boxes). In addition, two of the six residues described to bind the 9-cis bond of violaxanthin and the near methylcyclohexane are highly conserved among the sequences. This is the case of the two conserved Phe (F52 and F96). Meanwhile the other four residues vary in amino acid type, but their hydrophobic character is maintained: Met (M357) is changed to Ile or Leu, Val (V403) for Ale or Phe, Trp (W426) for Met or Ile, and finally Pro (P427) for Ala (Figure 2, red arrows). On the other hand, all the residues that coordinate Fe^{2+} (H223, H272, H337 and H515) (Figure 2, light blue arrows) and the amino acids stabilizing the His (E455) (Figure 2, blue arrows) are highly conserved between the sequences. The residues that bind the isoprene chain are also highly conserved between the sequences, except for FcCCD4. Only Glu (E189) is conserved throughout all sequences, meanwhile replacements of Ala (A139) for Val, Ile (I140) for Phe, Leu (L143) for Phe, Asp (D190) for Ser, Met (M270) for Leu, and Phe (F289) for Met are shown in FcCCD4 (Figure 2, green arrows).

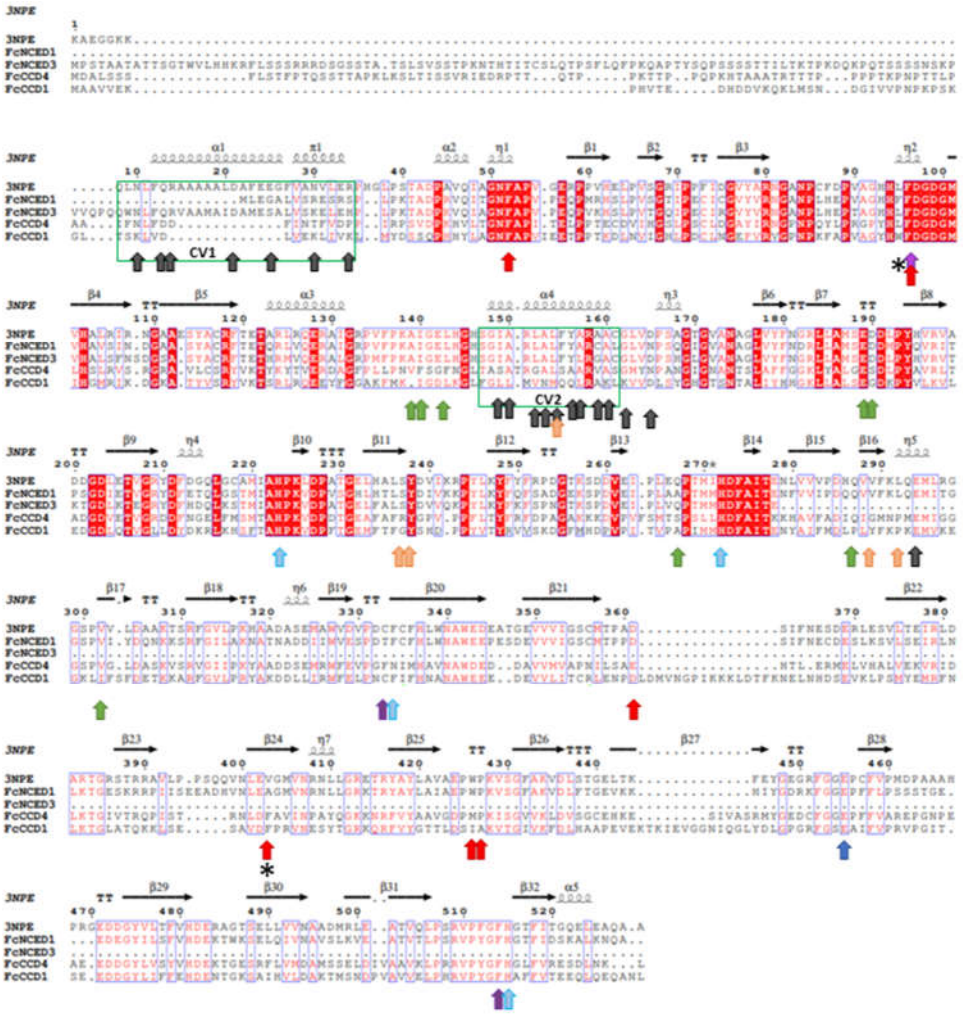

Figure 2. Alignment of deduced full-length amino acid sequences of FcNCED/CCD family. Amino acid sequences of FcNCED/CCDs and ZmVP14, an NCED-like protein (PDB code: 3NPE), were aligned using ESPript: gaps are indicated by dots, letters with red background are identical amino acids, and red letters are similar amino acids. The two cleavage sites (CV1-CV2) are indicated in boxes and correspond to two antiparallel α-helix regions. Red arrows indicate the binding site for 9-cis-

Preprints (www.preprints.org) | NOT PEER-REVIEWED | Posted: 19 April 2023 doi:10.20944/preprints202304.0574.v1

violaxanthin at 9-cis bond and the near methylcyclohexane; light-blue arrows indicate binding site for Fe^{2+}; blue arrows indicate amino acids helding the histidines which binds Fe; green arrows indicate binding site for 9-cis-violaxanthin at isoprene chain; orange arrows indicate binding site for 9-cis-violaxanthin at methylcyclohexane; purple arrow indicates binding site for 9-cis-violaxanthin at carotenoid section between C9-C15; black arrows indicate amino acids which interact with cell membrane; asterisks indicate amino acids that differentiate NCED and CCD (information obtained from [31]). Sequences were aligned using MAFFT version 7.

There are five residues which have been described to bind the methylcyclohexane group, and only one of them is conserved among the FcNCED/CCD sequences: Met (M295). For the remaining 4 residues, high variability is detected but maintain a high degree of hydrophobicity character (Figure 2, orange arrows). The residues that bind the carotenoid section between C9-C15 are also highly conserved between the sequences, being Phe in all sequences (F97, F336 and F514) except for *FcCCD4* which in replacement of F336 there is a Met (Figure 2, purple arrow).

Importantly, two amino acid residues have been described as key to differentiate between NCED and CCD (obtained from [31]). Those residues are Leu (L95 in 3NPE crystal) and Val/Ala/or Ile (V403 in 3NPE crystal) which are replaced by a Trp (W95) and a Phe (F403) in CCDs (Figure 2, asterisks). The sequences of FcNCED3 and FcCDD1 accomplish with bibliography, but FcNCED1 and FcCCD4 present different expected residues in location 95. FcNCED1 presents a Phe (F95) instead of the expected Leu for NCED activity, and FcCCD4 displays a Leu (L95) instead of the expected Trp for CCD.

2.2. Identification of FcPYR/PYL family genes and analysis of amino acid sequences

The search for *PYR/PYL* genes within the *F. chiloensis* transcriptome allows the identification of one *PYR* and five *PYLs* sequences (*FcPYR1, FcPYL2, FcPYL4, FcPYL8, FcPYL9, FcPYL12*) (Table 2). The sequences were named in accordance to *F. vesca* sequences. Their coding sequences contain the conserved domain described as 'Polyketide cyclase/dehydrase and lipid transport', which is present in most of the sequences, except for *FcPYL2*.

Table 2. Analysis of functional domains of deduced FcPYR/PYL amino acid sequences using PFAM database.

Gene	Transcript ID	Domain type	Seq length (aa)
FcPYR1	comp13086_c0_seq1	Polyketide cyclase/dehydrase and lipid transport	216
FcPYL2	comp7632_c0_seq1	ND	93
FcPYL4	comp22550_c0_seq1	Polyketide cyclase/dehydrase and lipid transport	218
FcPYL8	comp2447_c0_seq3	Polyketide cyclase/dehydrase and lipid transport	189
FcPYL9	comp3997_c0_seq2	Polyketide cyclase/dehydrase and lipid transport	121
FcPYL12	comp2932_c0_seq1	Polyketide cyclase/dehydrase and lipid transport	167

ND, not determined.

Preprints (www.preprints.org) | NOT PEER-REVIEWED | Posted: 19 April 2023 doi:10.20944/preprints202304.0574.v1

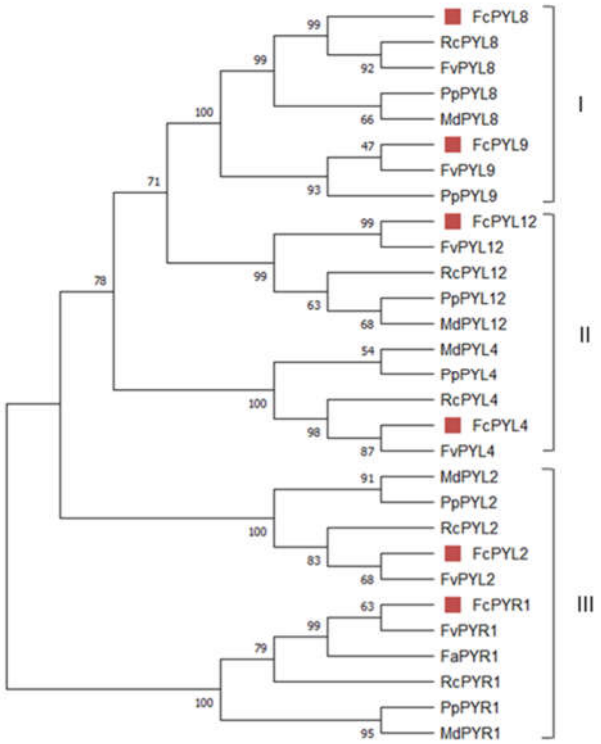

Figure 3. Phylogenetic analysis of *FcPYR* and *FcPYLs* proteins. Different *F. chiloensis* sequences (6) were aligned with other 23 sequences from *F. x ananassa* (1), *M. domestica* (5), *R. chinensis* (5), *P. persica* (6) and *F. vesca* (6). The phylogenic tree was built using the Neighbor-Joining method with bootstrap consensus tree inferred from 5000 replicates. The list of protein sequences employed in the analysis, including Genbank accession numbers, is shown in Table S2.

The phylogenetic analysis grouped them into three subfamilies (I-III). As the nomenclature used to name each subfamily is not consistent in literature, we decided to name them as reported by [32], based in *A. thaliana*. *FcPYR1* and *FcPYL2* belong to subfamily III, *FcPYL4* and *FcPYL12* are members of subfamily II (separated into two clades), meanwhile *FcPYL8* and *FcPYL9* belongs to subfamily I, also known as the AtPYL8-like subfamily (Figure 3).

A comparative alignment was performed between PYR/PYLs amino acid sequences of *F. chiloensis* and that of AtPYL2, whose 3D structure has been analyzed (PDB code: 3KAZ) (Figure 4) [33]. The alignment indicated the existence of important domains for these ABA receptors. The four connecting loops (CL1-CL4) which have been described as the interaction domains with ABA are highly conserved within the sequences, except for CL1 which is present in some of them (FcPYR1, FcPYL4 and FcPYL8) and CL2 which is absent in FcPYL2. CL2 has been described as a gate and latch structure [34].

Preprints (www.preprints.org) | NOT PEER-REVIEWED | Posted: 19 April 2023 doi:10.20944/preprints202304.0574.v1

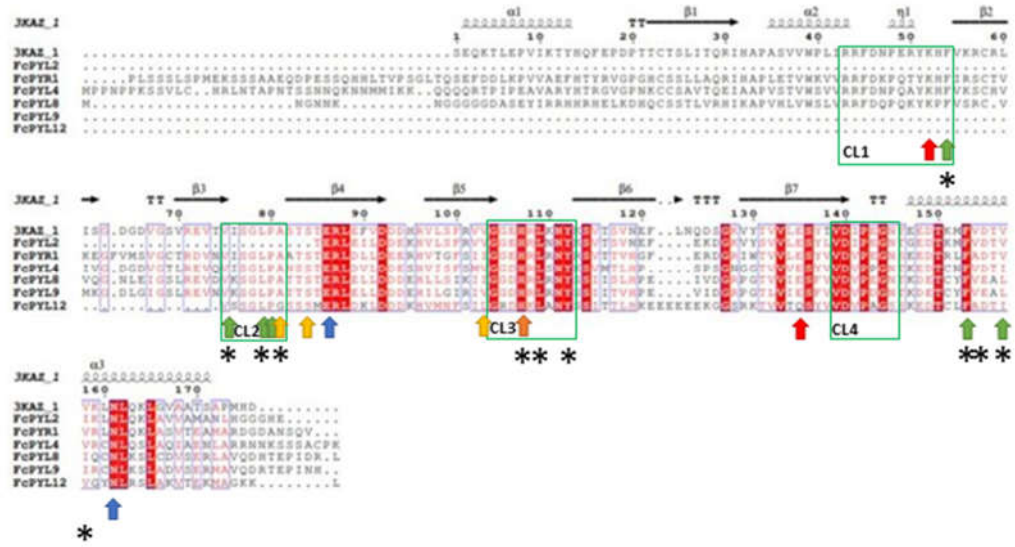

Figure 4. Alignment of deduced full-length amino acid sequences of FcPYR/PYL family**.** Amino acid sequences of FcPYR/PYLs and AtPYL2 (PDB code: 3KAZ) were aligned using ESPript: gaps are indicated by dots, letters with red background are identical amino acids, and red letters are similar amino acids. The four connecting loops (CL1-CL4) are indicated in boxes and correspond to interaction domains with ABA. Red arrows indicate the binding site for carboxyl group of ABA, blue arrows indicate hydrogen bonds with the carboxyl group of ABA, green arrows indicate binding site for methyl group of ABA, yellow arrows indicate binding site for dimethyl group of ABA, asterisks indicate amino acids present in the hydrophobic pocket, and the orange arrow indicates the binding site for PP2C protein (information captured from [33,34]). Sequences were aligned using MAFFT version 7.

Furthermore, the sequences contain the amino acid residues involved in ABA and PP2C binding. The protein sequences coded by *FcPYR1, FcPYL4* and *FcPYL8* present a highly conserved Lys residue (K52) that binds to the carboxyl group of ABA (Figure 4, red arrow). All sequences possess a highly conserved Glu residue (E135) that also binds to a carboxyl group of ABA, except for *FcPYL12* which presents a Gln (Figure 4, red arrow). All sequences share two highly conserved residues, Glu (E86) and Asn (N161), which interacts through hydrogen bonds with the carboxyl group of ABA (Figure 4, blue arrow).

Five of the six residues that bind to the methyl group of ABA are highly conserved between the sequences: Phe (F54), Val (V75), Leu (L79), Pro (P80) and Phe (F153); but the sixth residue, Val (V157), may vary for a Leu or Ile among the different *FcPYR/PYL* proteins (Figure 4, green arrow). Some of these residues are also involved in the hydrophobic pocket (F54, V75, L79, F153), in addition to His (H107), Leu (L109) and Tyr (Y112) which hold a high degree of conservation; however other residues are modified in this hydrophobic pocket, Ala (A81) for Gly, Val (V157) for Leu or Ile, and Val (V158) for Ile (Figure 3, asterisk).

There are three residues that have been identified to bind the dimethyl group of ABA (Ala 81, Ser 84, Val 102) (Figure 4, yellow arrow), which are mostly conserved among *F. chiloensis* sequences. Few changes exists as there is a Gly instead of Ala81 in FcPYL12, and Val102 may vary for Ile or Met. Finally, a highly conserved His among sequences (H107) allows the interaction of *PYR/PYL* with *PP2C* (Figure 4, orange arrow).

2.3. Expression analysis of ABA biosynthesis related genes in F. chiloensis

The relative expression level of ABA biosynthesis related genes, *FcNCED* and *FcCCD*, was quantified by RT-qPCR in different vegetative tissues. A high relative expression level of *FcNCED1* transcripts was noticed in roots, and a middle expression level in runners and low level in the other vegetative tissues analyzed (Figure 5A). In the case of *FcCCD1* transcripts, high expression level was

Preprints (www.preprints.org) | NOT PEER-REVIEWED | Posted: 19 April 2023 doi:10.20944/preprints202304.0574.v1

detected in flowers and low expression level in the other vegetative tissues (Figure 5B). On the other hand, transcripts level for *FcNCED3* and *FcCCD4* were extremely low in the vegetative tissues under study.

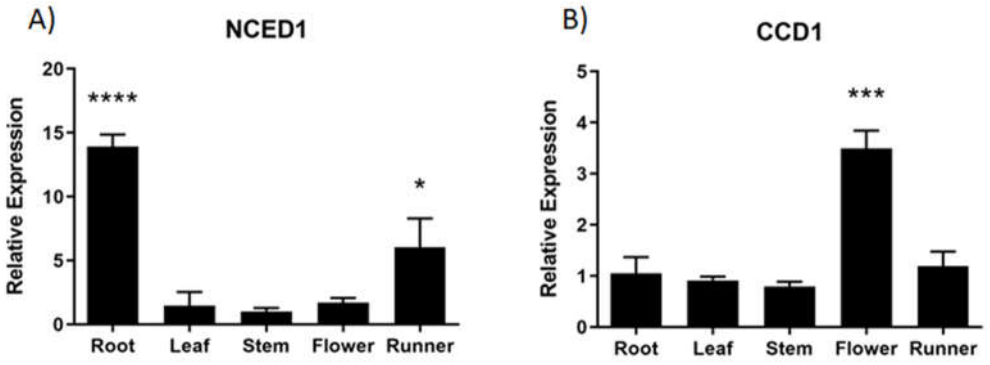

Figure 5. Relative expression levels of *FcNCED/CCDs* in several *F. chiloensis* vegetative tissues. Expression levels of *FcNCED1* (A) and *FcCCD1* (B) were determined by RT-qPCR. Values were first normalized against the expression data of *FcDBP*, and then calibrated against stem tissue in the case of *FcNCED1* and root tissue in the case of *FcCCD1*, with a nominal value of 1. Each value corresponds to the mean ± SE of three independent RNA extractions and qPCR analysis using three technical replicates. Asterisks indicate significant differences compared to calibrated tissue (*p<0.05, **p<0.01, ***p<0.001, or ****p< 0.0001; One-way ANOVA with Dunnet correction post-hoc).

In development fruit tissue, the relative accumulation of *FcNCED1* transcripts displays an increment during development with a maximum value at C3 stage (Figure 6A). *FcNCED3* shows an early increment at C2 stage which decay over time (Figure 6B). *FcCCD1* displays the same expression profile as *FcNCED3* (Figure 6C). Finally, *FcCCD4* is mainly expressed at C3 and C4 stages with no significant differences among those stages (Figure 6D).

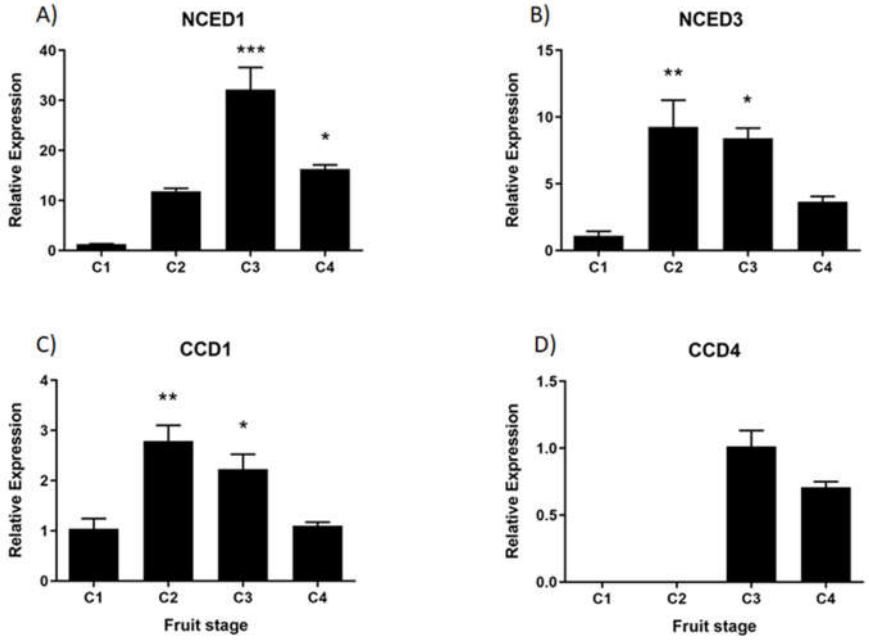

Figure 6. Relative expression levels of *FcNCED/CCDs* in *F. chiloensis* developing fruit. Expression levels were determined by RT-qPCR: (A*) FcNCED1*, (B) *FcNCED3*, (C) *FcCCD1* and (D) *FcCCD4*. Values were first normalized against the expression data of *FcDBP*, and then calibrated against the expression of C1 stage with a nominal value of 1 or C3 in the case of *FcCCD4*. Each value corresponds to the mean ± SE of three independent RNA extractions and three technical replicates. Asterisks

Preprints (www.preprints.org) | NOT PEER-REVIEWED | Posted: 19 April 2023 doi:10.20944/preprints202304.0574.v1

indicate significant differences compared to C1 stage (*p<0.05, **p<0.01, ***p<0.001; One-way ANOVA with Dunnet correction post-hoc).

Heatmap analysis of non-calibrated qPCR values for ABA biosynthesis genes indicates that the expression level of *FcNCED1* was higher than for the other genes in fruit samples (Figure 7). In comparison, the expression level in fruit tissues followed the order *FcNCED1* > *FcCCD1* > *FcNCED3* > *FcCCD4*. In vegetative tissues, *FcNCED1* is highly expressed in roots, and *FcCCD1* in flowers.

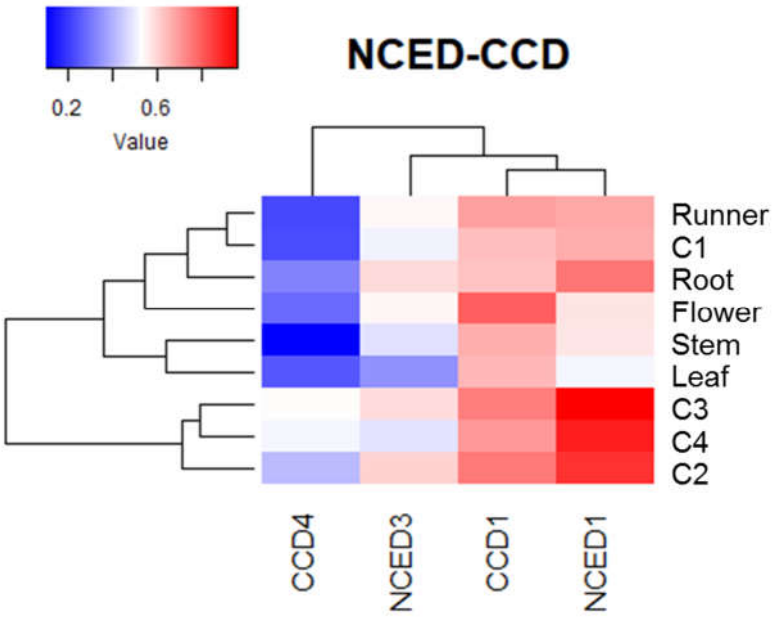

Figure 7. Heatmap analysis of *FcNCED/CCD* transcripts, clustered in based of their accumulation profile and tissue specificity. The columns of the heatmap represent genes and the rows correspond to samples. Each cell is colorized based on the expression level of a particular gene in a certain sample. The values used in the analysis correspond to the expression level of each *FcNCED/CCD* gene without calibration.

2.4. Expression analysis of ABA receptor genes during development of F. chiloensis fruit and vegetative tissues

The expression of *FcPYR/FcPYLs* was quantified by qPCR analysis in different vegetative tissues in order to provide a molecular evidence of ABA perception (Figure 8). Among the six different genes analyzed, only five of them were transcribed in the different vegetative tissues under analysis; extremely low expression level was detected for *FcPYR1*. High relative expression level of *FcPYL2* and *FcPYL12* was detected in roots and flowers, and middle to low expression in runners, leaves, and stem. A relatively high level of transcripts accumulation was also observed for *FcPYL4* in roots. In the case of *FcPYL8* and *FcPYL9* there were no significant differences in transcripts accumulation among the vegetative tissues analyzed. Heatmap analysis were built with non-calibrated expression data and indicated that the most expressed gene among vegetative tissues is *FcPYL8*, middle-high expression level in the case of *FcPYL4* and *FcPYL12*, and middle level for *FcPYL9* (Figure 9).

Preprints (www.preprints.org) | NOT PEER-REVIEWED | Posted: 19 April 2023 doi:10.20944/preprints202304.0574.v1

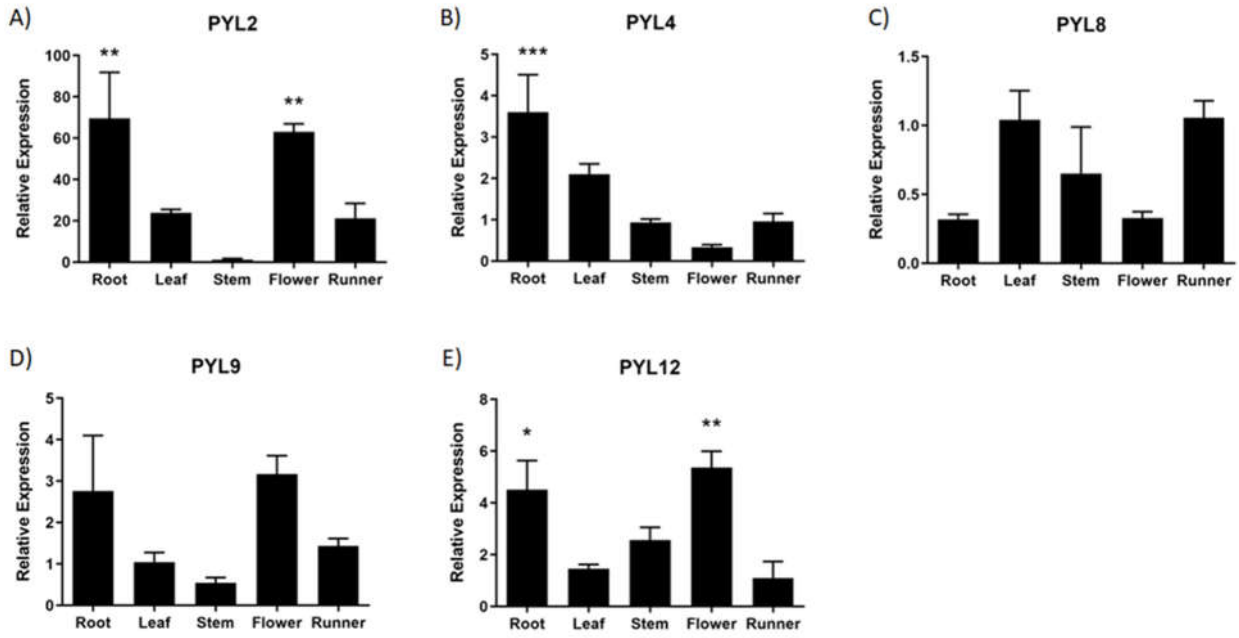

Figure 8. Relative expression levels of *FcPYR/PYLs* in several *F. chiloensis* vegetative tissues. Expression analyses were performed by RT-qPCR. Values were initially normalized against the expression data of *FcDBP*, and then calibrated against a selected tissue (stem in A and B; leaf in C and D; runner in E) with a nominal value of 1. Each value corresponds to the mean ± SE of three independent RNA extractions and three technical replicates. Asterisks indicate significant differences compared to calibration tissue (*p<0.05, **p<0.01, ***p<0.001; One-way ANOVA with Dunnet correction post-hoc).

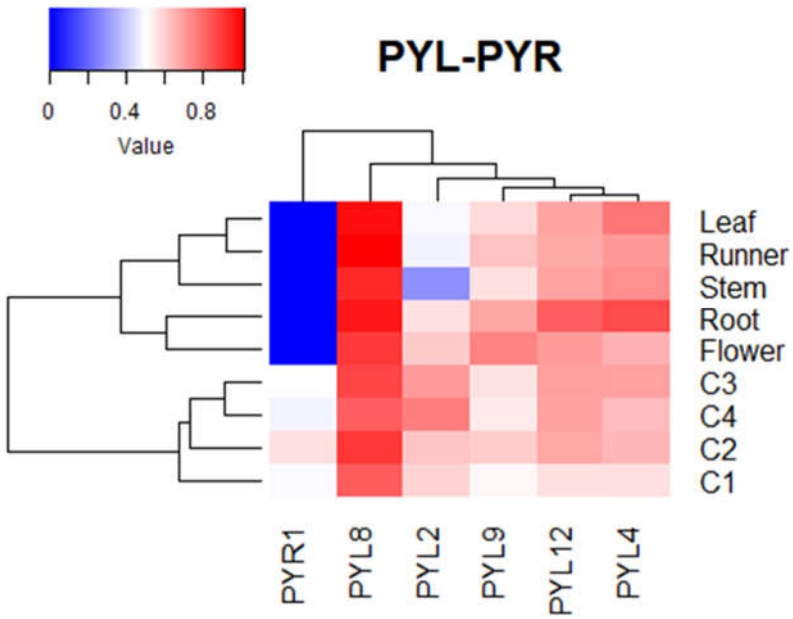

Figure 9. Heatmap analysis of *FcPYR/PYL* transcripts, clustered in based of their accumulation profile and tissue specificity. The columns of the heatmap represent genes and the rows correspond to samples. Each cell is colorized based on the expression level of each gene in a particular sample. The values used in the analysis correspond to expression values of *FcPYR/PYLs* without calibration.

During development and ripening of *F. chiloensis* fruit there are significant changes in the expression level of all *FcPYL/PYR* genes under study (Figure 10). In *FcPYL* genes there is a clear

Preprints (www.preprints.org) | NOT PEER-REVIEWED | Posted: 19 April 2023 doi:10.20944/preprints202304.0574.v1

increment in the level of transcripts along fruit development and ripening, although different profiles can be observed. In the case of *FcPYL2* there is a clear increment in transcripts from stage 3, with maximum values at stage 4. In the case of *FcPYL4* there is also a sudden rise at stage 3 but decreases after that. In the case of *FcPYL9* the rise in transcripts is observed from stage 2, reaching the maximum value at stage 3 and then decreases at stage 4. And in the case of *FcPYL12* a rise was observed at stage 2 and the level was maintained until the end of ripening. In the case of *FcPYR1* a completely different expression profile was observed, with a rise in expression between stage 1 and 2, followed by a reduction at stage 3 and 4. Heatmap analysis indicated that *FcPYL8* is the most expressed gene in ripe fruit tissues, followed by *FcPYL2*, *FcPYL12*, *FcPYL4*, and *FcPYL9* (Figure 10). The expression level of *FcPYR1* is very low compared to the other *PYL* genes.

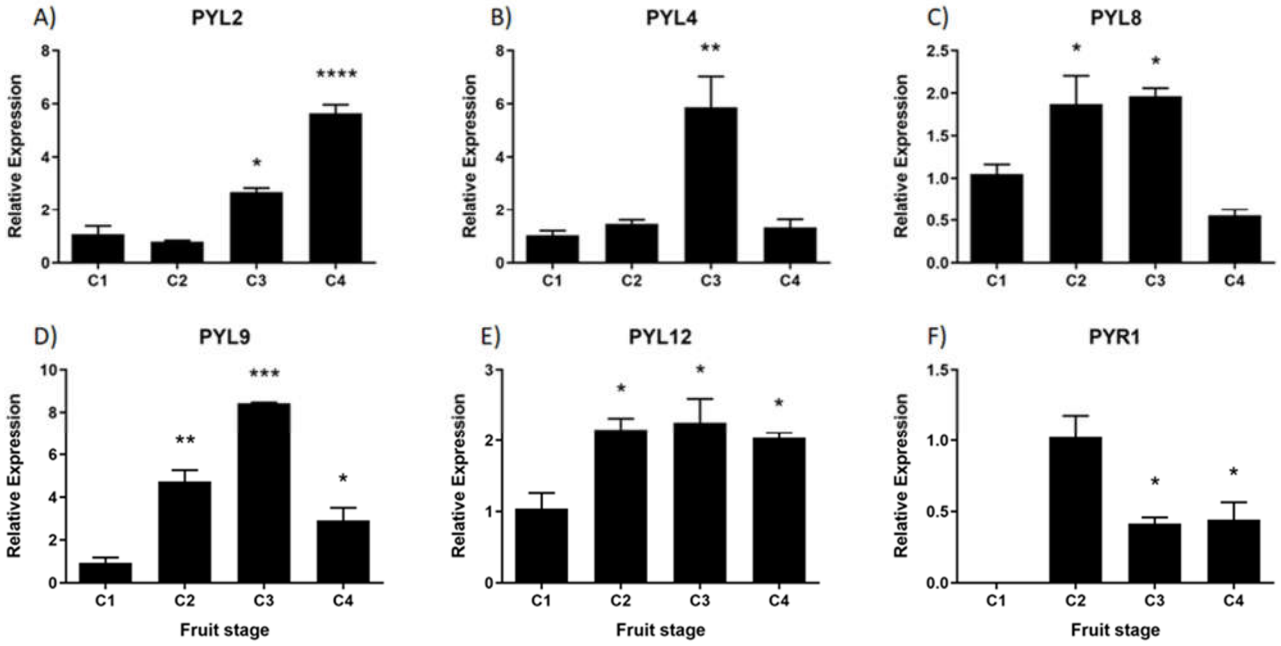

Figure 10. Relative expression levels of *FcPYR/PYL*s in *F. chiloensis* developing fruit. Expression analyses were performed by RT-qPCR. Values were first normalized against the expression data of *FcDBP*, and then calibrated against the expression of C1 stage with a nominal value of 1 or C2 in the case of *FcPYR1*. Each value corresponds to the mean ± SE of three independent RNA extractions and three technical replicates. Asterisks indicate significant differences compared to C1 stage (*p<0.05, **p<0.01, ***p<0.001, or ****p< 0.0001; One-way ANOVA with Dunnet correction post-hoc).

2.5. During fruit development ABA levels correlates with ABA biosynthesis genes and ABA receptor genes.

ABA levels during development and ripening of *F. chiloensis* fruit have been reported earlier [11], showing an increment as fruit ripens, with higher levels at stages 3 and 4. Pearson correlation values indicate a direct correlation between ABA levels during fruit development and the expression level of ABA biosynthesis genes such as *FcNCED1* (r= 0.86) and *FcCCD4* (r=0.99) (Figure 11). This indicates that *FcNCED1* and *FcCCD4* may be involved in the biosynthesis of ABA during ripening of *F. chiloensis* fruit. In addition, the increment in ABA is coincident with the increase expression of *FcPYL2* (r=0.70) and FcPYL4 (r=0.64), suggesting their participation in ABA sensing.

Positive correlations were found between the expression levels of the different genes: *FcPYL4* correlates with *FcNCED1* (r=0.92); *FcPYL8* correlates with *FcNCED3* (r=0.80) and *FcCCD1* (0.92); *FcPYL9* correlates with *FcNCED3* (r=0.99) and *FcCCD1* (r=0.98); *FcPYR1* correlates with *FcCCD1* (0.83); *FcNCED1* correlates with *FcCCD4* (0.90); *FcNCED3* correlates with *FcCCD1* (0.95). Interestingly, the only negative correlation was found between *FcPYL2* and *FcPYL8* (r=-0.80).

Preprints (www.preprints.org) | NOT PEER-REVIEWED | Posted: 19 April 2023 doi:10.20944/preprints202304.0574.v1

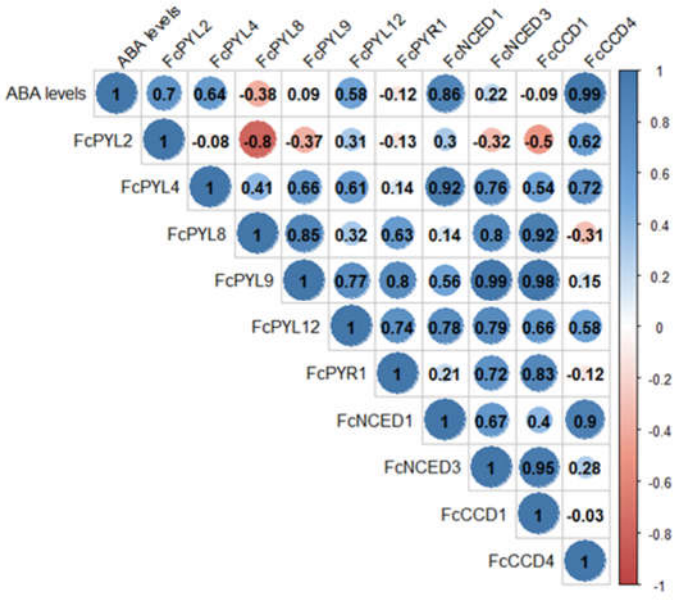

Figure 11. Pearson correlation analysis between ABA levels during fruit development, ABA biosynthesis genes and ABA receptor genes. Raw expression values of each gene and ABA level data from the four development and ripening stages of *F. chiloensis* fruit were analyzed in order to find correlations.

3. Discussion

Carotenoid cleavage dioxygenases (CCDs) are a family of enzymes that catalyzes the cleavage of carotenoids into smaller apocarotenoids, molecules with relevant properties including pigments, flavor and aroma compounds, and plant growth regulators such as vitamin A, ABA and strigolactone [35,36]. The CCD gene family comprises CCD and NCED subfamilies. Importantly, NCED can catalyze the cleavage of 11, 12 double bond of violaxanthin (C40) or neoxanthin (C40) to form xanthoxin (C15), the precursor of ABA. The reaction carried out by NCED is considered the rate-limiting step in ABA biosynthesis.

In *Fragaria chiloensis* two *NCEDs* and two *CCDs* were identified within the transcriptome prepared from fruit samples [37]. In general, the number of *CCD* genes identified in the genome of different fruit species is reduced compared to the number described in non-fruit species (30 in oilseed rape, 19 in tobacco) [35]. In the genome of watermelon (*Cucumis lanatus*), melon (*C. melo*) and cucumber (*C. sativus*) a recent report indicated the existence of 10, 9 and 9 *NCED/CCD* protein sequences, respectively [35]. In all these cucurbitaceae species there are 4 *NCED* sequences and 5 or 6 *CCDs*. In litchi (*Litchi chinensis*), 15 *LcCCO* genes were identified in its genome, 3 *NCEDs* and 12 *CCDs* [36]. In tomato, 7 *CCD* sequences have been described within its genome [38]. In comparison, in Arabidopsis a total of 9 members of the *CCD* family have been reported, divided into 4 *CCDs* and 5 *NCEDs* [39]. Therefore, the number of *CCD* members in *F. chiloensis* is reduced compared to other fruit species, but as the search has been restricted to a fruit transcriptome there may be other sequences waiting to be discovered.

Several studies suggested that different *CCD* subfamilies exhibit different roles within the plant kingdom. For example, *CCD1* plays important roles in aroma and flavor of horticultural products as catalyzes the formation of α-ionone, β-ionone and geranylacetone [40,41]. *CCD4* contributes to color formation in flower petals and fruit peel, and also aroma production [42-48]. *CCD7* and *CCD8* seem to participate in the biosynthesis of the hormone strigolactone, which could control shoot branching, reproductive development and plant responses to drought and salt stress [49-52]. Finally, *NCED* subfamily is involved in ABA biosynthesis, and closely involved in fruit development and ripening. In commercial strawberry *FaNCED1* has been demonstrated to be crucial for ABA biosynthesis, as RNAi constructs promoted a dramatic reduction in ABA content that reduced development of red

 doi:10.20944/preprints202304.0574.v1

color [12], and the phenotype was reverted by the application of exogenous ABA. Similarly in grape [53], sweet cherry [54] and litchi fruit [55] ABA accelerated the accumulation of anthocyanins by increasing the expression of *NCED*.

In litchi *LcCCD4s*, *LcCCD1*, *LcNCED1* and *LcNCED2* might participate in postharvest storage of the fruit and peel coloration [36]. The expression of *LcNCED1* in fruits was consistent with the accumulation of ABA during the ripening of litchi [56]. In peach and grape fruits *PpNCED1* and *VvNCED1* transcripts increase at early stages of ripening, which initiates ABA biosynthesis and ABA accumulation [57]. In *Citrus clementina*, the expression of *CcNCED5* increases at color break and remains high at the ripe stage in parallel to ABA levels, suggesting a role in the ripening of mandarin fruit [58].

In melon the expression of *CmCCD1* was upregulated during development of the fruit and seems to participate in aroma formation [59]. In addition, *CmCCD1* was upregulated by ABA, and other stress conditions such as drought and salt [35]. The expression of *CmNCED3* was upregulated in melon leaves under a series of abiotic stress (salt, cold, drought), indicating that plays an important role in stress [35]. Finally, *CmNCED5s* are highly expressed in flowers and play crucial roles in flower growth and development [35].

From the *FcNCED/CCD* sequences identified in *F. chiloensis*, all of them were detected in fruit tissues, albeit with different profiles. This is not surprising as the sequences were obtained from a fruit transcriptome. Only *FcNCED1* and *FcCCD1* were detected in vegetative tissues: *FcNCED1* in roots and runners, and *FcCCD1* mostly in flowers.

The phylogenetic analysis grouped *FcNCED1* in the same branch with *FaNCED1* and *FvNCED1*. Our data indicates that the expression level of *FcNCED1* increases as the ripening of the fruit is taking place. This also correlates with the increment in ABA observed in the fruit during development. Interestingly this gene is mainly expressed in fruit tissues, with low expression level in roots. All these evidences indicates that *FcNCED1* is the orthologous of *FaNCED1*, a gene which has been demonstrated to be involved in ABA biosynthesis during ripening of *F. x ananassa* fruit whose repression by RNAi avoided the biosynthesis of ABA [12]. Importantly, the expression of *FcNCED1* has been reported to be induced in fruit by ABA treatment [11].

The alignment of deduced amino acid sequences indicated that FcNCEDs and FcCCDs share important domains related to activity. The amino acid residues identified as part of cleavage domains are mostly conserved. Two amino acids seems to discriminate between NCED and CCD proteins: L95 and V403 from ZmVP14. The corresponding residues in FcNCED3 and FcCCD1 are in agreement with hypothetic differentiation for activity, however in the case of FcNCED1 and FcCCD4 the residue at location 95 is not the expected. FcNCED1 contains a Phe instead of the expected Leu, and FcCCD4 contains a Leu instead of Trp. Nevertheless, the changes in amino acids do not interfere with their character, as Phe, Leu and Trp are nonpolar hydrophobic residues. Interestingly, the same Phe identified in FcNCED1 exists in FvNCED1 and AtNCED3, and in the case of FcCCD4 the Leu in position 95 also exists in FvCCD4, RrCCD4, PaCCD4 and MdCCD4. Therefore the discrimination between these two activities requires further studies.

The search for ABA receptor sequences within the *F. chiloensis* fruit transcriptome provided the identification of one *PYR* and five *PYLs* sequences. The translated amino acid sequences displayed the connecting loops required for the interaction with ABA, and most of the residues involved in ABA and PP2C binding. The phylogenetic analysis grouped them into three subfamilies that correlates well with the number of subfamilies reported in many species. As in Arabidopsis, subfamily II includes FcPYL4 in one clade and FcPYL12 in another. Interestingly this second clade is missing in monocot species, and also in some dicots such as tomato and citrus [32], but it is present in *F. chiloensis*, a Rosaceae species. The three PYR/PYL families have arisen during evolution; the latest to emerge is subfamily III which is present only in angiosperms [40]. Subfamilies I and II are composed of monomeric receptors, with high basal activity, and require only a low level of ABA to induce PP2C inhibition, while subfamily III receptors are dimeric in solution and have low basal activity [60].

Preprints (www.preprints.org) | NOT PEER-REVIEWED | Posted: 19 April 2023 doi:10.20944/preprints202304.0574.v1

All *FcPYR/PYLs* were expressed in *F. chiloensis* fruit tissues, and all of them except for *FcPYR1* were expressed in vegetative tissues. *FcPYL8* was the most expressed gene in vegetative tissues. Different expression profiles were obtained for *FcPYR/PYLs* in ripening fruit. Of interest is the expression of *FcPYL2* and *FcPYL4* along the ripening progress, as their expression followed the increment in ABA level reported in the fruit, suggesting their participation in ABA perception. Nevertheless, *FcPYL2* does not contain CL2 which is crucial for ABA interaction.

The expression of PYR/PYL gene family has been analyzed during ripening in different fruits species. In cucumber, *CsPYL2* was expressed at high level during fruit ripening, with a peak of expression between turning and ripe stages, coincident with the highest level of ABA content in the fruit, suggesting its participation in ABA perception during fruit ripening [61]. In Chinese white pear, from the eleven *PbrPYL* genes identified in its genome, seven of them, which were distributed within the three subfamilies, were expressed in ripe fruit (*PbrPYL1/4/5/6/7/8/9*) [61]. In grapes (*Vitis vinifera*), from the eight PYL genes identified in the genome, two of them have a particular expression profile of interest for fruit ripening, as *VvPYL1* and *VvPYL8* significantly increased from fruit set till the ripening stage [62]. Those two genes can be classified in subfamily I.

In citrus genome, 11 *PYL* sequences have been identified [32]. Expression analysis in fruit performed in only 6 *CsPYLs* shown that *CsPYL9* belonging to subfamily I was the most expressed during sweet orange development and ripening [63].

In tomato, a climacteric fruit, two of the fourteen *SlPYL* genes identified displayed an expression peak at breaker stages, when ripening is starting, and reported as candidates to regulate fruit ripening [64]. These two genes belong to subfamilies I and II according to our nomenclature. A recent study, confirm that among the 14 *SlPYLs*, the expression level of *SlPYL1* was the highest, and the expression patterns of *SlPYL1*, *SlPYL4*, and *SlPYL9* agreed with the ABA accumulation in fruit during development [65]. Interestingly, *SlPYL9* which is closest to monomeric *AtPYL4* and therefore belongs to subfamily II, seems to have a specific role in fruit development and ripening. The overexpression of *SlPYL9* accelerated the ripening of the fruit, meanwhile RNAi lines showed a delay in ripening [65].

It has been proposed that *PYR/PYL* genes grouped into the same subfamily may perform similar functions, however as described, members of the three subfamilies have been identified with a role during ripening in several fruit species (*F. chiloensis*, tomato, Chinese pear, grapes and citrus), and therefore, this statement is not fully true in the case of fruit ripening.

In conclusion, *FcNCED1* is expressed with an increasing pattern during ripening of *F. chiloensis* fruit which correlates with the ABA levels reported for the fruit. In addition, the gene also increments its expression in response to ABA. On the other hand, *FcPYL4* from subfamily II displays an expression profile which may explain ABA perception. These two genes, *FcNCED1* and *FcPYL4*, might be in charge of ABA biosynthesis and ABA perception during the ripening of *F. chiloensis* fruit.

4. Materials and Methods

4.1. Plant material

White Chilean strawberry fruit (*F. chiloensis* (L.) Mill. subsp. *chiloensis* f. *chiloensis* Staudt) and vegetative tissues (leaves, flowers, runners, stem, and roots) were collected from plants grown in a commercial field at Purén, The Araucanía Region, Chile. The fruit was segregated into four different stages, C1, C2, C3 and C4, as recently reported [11]. Three pools of fruit tissue were prepared including 5 fruit from each stage. Fruit and vegetative tissue samples were frozen in liquid nitrogen, converted into a powder with the help of a mortar and pestle, and then stored at -80 °C until use.

4.2. F. chiloensis gene sequences

Genes annotated as *NCED/CCD* and *PYR/PYL* were selected from the Genome Database of Rosaceae [66] using *Malus domestica*, *Prunus persica*, *Rosa chinensis* and *F. x ananassa* as reference species. Then, a comparative mapping of selected sequences and a *F. chiloensis* transcriptome was carried out as a way to identify their orthologs [37]. Sequences were aligned using MAFFT version 7

Preprints (www.preprints.org) | NOT PEER-REVIEWED | Posted: 19 April 2023 doi:10.20944/preprints202304.0574.v1

(https://mafft.cbrc.jp/alignment/server/). The search provides one ortholog sequence for *PYR*, five for *PYL*, two for *NCED* and two for *CCD*. The sequences were named based on the best alignment against NR database.

4.3. Phylogenetic analysis and motif analysis

Phylogenetic analyses were performed to analyze the evolutionary relationship of NCED - CCD and PYR – PYL sequences. The analyses were conducted by MEGA software v10.1. Sequence alignment was performed through CLUSTAL W method and the phylogenetic tree by Neighbor joining algorithm with 5000 bootstrap replicates.
The amino acid sequences deduced from *F. chiloensis* genes were analyzed using Pfam prediction, searching for conserved evolutionary domains related to ABA.

4.4. RNA extraction and expression analysis by Real Time PCR (qPCR)

The procedure described in [11] was employed to extract RNA and to perform cDNA synthesis from fruit/tissue samples. Specific primers for qPCR analysis are listed in Table 3. qPCR reactions were carried out in triplicates, and employing three independent cDNA preparations from each biological sample. Relative expression levels correspond to the mean of three biological replicates ± SE normalized against the expression level of *FcDBP* (DNA binding protein) (constitutive gene) [67]. C1 fruit stage was employed as calibrator for fruit samples, and the tissue with the lowest expression was employed as calibrator for the analysis of vegetative tissues. Asterisks indicate significant differences among fruit stages or different tissues.

Table 3. Nucleotide sequence of the primers used in the qPCR analyses (Tm of 60 °C).

Gene		Sequence (5′ → 3′)	Efficiency
FcNCED1	Fw	GATCTACCTTGGCGAAACCA	90.0%
	Rv	GAGGCGGATCATGTGAACTT	
FcNCED3	Fw	ACGACTTCGCCATTACCG	92.1%
	Rv	AGCATCGCTCGATTCT	
FcCCD1	Fw	GCCAAGCATATGACACTCCTC	98.0%
	Rv	TCCTCGTTAGAAGGCCTGAA	
FcCCD4	Fw	CATTCCCGACCAAGATAGGA	94.3%
	Rv	GCCGTCCTTTGAGTAAACC	
FcPYL2	Fw	GCCATGGTGGTCAACTGTTA	100.5%
	Rv	CTGGGATTCTGGGGTACAC	
FcPYL4	Fw	ATGCCTCCCAACCCACCCAA	104.0%
	Rv	CGCTGCTGCTGCTGCTTCTT	
FcPYL8	Fw	TGAAGCTTCCGAGCTTTCAT	92.1%
	Rv	GGTCCTTAAACTTTGACGGAAG	
FcPYL9	Fw	GATGCACCTGCTAACAAAAGG	90.1%
	Rv	CAATCGTGTTTCTCATTTGTGC	
FcPYL11	Fw	GAAAGGATGGCTGGTAATTGA	91.0%
	Rv	CGCTACAACAAGAAGTCAAGAA	
FcPYL12	Fw	TTTCCTATCCTGCTGCTGCT	96.1%
	Rv	GCTTAGAATCCGAAACGGACTA	
FcPYR1	Fw	GCTACCCAAATTGCTGAACC	99.3%
	Rv	GAATGACGAAAATGTCCTTGG	

4.5. Heatmap analysis

Heatmap analysis were generated using the open-source software R - graphic interface R-Studio (1.3.1093). The diagrams and dendrograms were obtained with the packages "gplots" and "corrplot" which are included in the R library.

4.6. Statistical analysis

For gene expression analysis a random design with 3 biological replicates and 3 technical replicates was employed. For comparisons of qPCR results one-way ANOVA was used with Dunnet correction post-hoc; differences were considered statistically significant when $p < 0.05$ (*), $p < 0.01$ (**), $p < 0.001$ (***), or $p < 0.0001$(****).

Supplementary Materials: Table S1: List of protein sequences employed in the phylogenetic analyses of *PYR/PYL*, including GenBank accession numbers; Table S2: List of protein sequences employed in the phylogenetic analyses of *NCED/CCD*, including GenBank accession numbers.

Author Contributions: The present work was conceived and designed by MAM-L, YS, EM-A and RH. YS and EM-A contributed collecting information and preparing figures. YS contributed with bioinformatics analyses. EM-A performed RT-qPCR analysis. MAM-L and RH participate in the writing and discussion of the manuscript. Each author participated sufficiently in the work to take public responsibility for appropriate portions of the content. All authors read, edited and approved the final manuscript.

Funding: This research was funded by ANID-FONDECYT grant number 1210948 and ANID-ANILLO grant ACT210025.

Institutional Review Board Statement: Not applicable.

Data Availability Statement: All data generated or analyzed during this study are included in this published article.

Acknowledgments: Thanks to Jocelyn Guajardo for her technical assistant and Rodrigo Lizana for given the first steps in the study of ABA biosynthesis pathway in *F. chiloensis*.

Conflicts of Interest: The authors declare no conflict of interest. The funders had no role in the design of the study; in the collection, analyses, or interpretation of data; in the writing of the manuscript; or in the decision to publish the results.

References

1. Figueroa, C.R.; Pimentel, P.; Gaete-Eastman, C.; Moya, M.; Herrera, R.; Caligari, P.D.S.; Moya-León, M.A. Softening rate of the Chilean strawberry (*Fragaria chiloensis*) fruit reflects the expression of polygalacturonase and pectate lyase genes. *Postharvest Biol. Technol.* **2008**, *49*, 210–220. https://doi.org/10.1016/j.postharvbio.2008.01.018.
2. Letelier, L.; Gaete-Eastman, C.; Peñailillo, P.; Moya-León, M.A.; Herrera, R. Southern species from the biodiversity hotspot of central Chile: A source of color, aroma, and metabolites for global agriculture and food industry in a scenario of climate change. *Front. Plant Sci.* **2020**, *11*, 1002. https://doi.org/10.3389/fpls.2020.01002
3. Molinett, S.A.; Alfaro, J.F.; Sáez, F.A.; Elgueta, S.; Moya-León, M.A.; Figueroa, C.R. Postharvest treatment of hydrogen sulfide delays the softening of Chilean strawberry fruit by downregulating the expression of key genes involved in pectin catabolism. *Int. J. Mol. Sci.* **2021**, *22*, 10008. https://doi.org/10.3390/ijms221810008
4. Giovannoni, J. Molecular biology of fruit maturation and ripening. *Annu. Rev. Plant Physiol. Plant Mol. Biol.* **2001**, *52*, 725–749. https://doi.org/10.1146/annurev.arplant.52.1.725
5. Moya-León, M.A.; Mattus-Araya, E.; Herrera, R. Molecular events occurring during softening of strawberry fruit. *Front. Plant Sci.* **2019**, *10*, 615. https://doi.org/10.3389/fpls.2019.00615
6. Symons, G.M.; Chua, Y.-J.; Ross, J.J.; Quittenden, L.J.; Davies, N.W.; Reid, J.B. Hormonal changes during non-climacteric ripening in strawberry. *J. Exp. Bot.* **2012**, *63*, 4741–4750. https://doi.org/10.1093/jxb/ers147
7. Jiang, Y.; Joyce, D.C. ABA effects on ethylene production, PAL activity, anthocyanin and phenolic contents of strawberry fruit. *Plant Growth Regul.* **2003**, *39*, 171–174. https://doi.org/10.1023/A:1022539901044
8. Opazo, M.C.; Figueroa, C.R.; Henríquez, J.; Herrera, R.; Bruno, C.; Valenzuela, P.D.T.; Moya-León, M.A. Characterization of two divergent cDNAs encoding xyloglucan endotransglycosylase/hydrolase (XTH) expressed in *Fragaria chiloensis* fruit. *Plant Sci.* **2010**, *179*, 479–488. https://doi.org/10.1016/j.plantsci.2010.07.018
9. Medina-Puche, L.; Blanco-Portales, R.; Molina-Hidalgo, F.J.; Cumplido-Laso, G.; García-Caparrós, N.; Moyano-Cañete, E.; Caballero-Repullo, J.L.; Muñoz-Blanco, J.; Rodríguez-Franco, A. Extensive transcriptomic studies on the roles played by abscisic acid and auxins in the development and ripening of strawberry fruits. *Funct. Integr. Genomics* **2016**, *16*, 671–692. https://doi.org/10.1007/s10142-016-0510-3

10. Mattus-Araya, E.; Guajardo, J.; Herrera, R.; Moya-León, M.A. ABA speeds up the progress of color in developing *F. chiloensis* fruit through the activation of *PAL*, *CHS* and *ANS*, key genes of the phenylpropanoid/flavonoid and anthocyanin pathways. *Int. J. Mol. Sci.* **2022**, *23*, 3854. https://doi.org/10.3390/ijms23073854
11. Mattus-Araya, E.; Stappung, Y.; Herrera, R.; Moya-León, M.A. Molecular actors involved in the softening of *Fragaria chiloensis* fruit accelerated by ABA treatment. *J. Plant Growth Regul.* **2023**, 42, 433-448. https://doi.org/10.1007/s00344–021–10564–3
12. Jia, H.-F.; Chai, Y.-M.; Li, C.-L.; Lu, D.; Luo, J.-J.; Qin, L.; Shen, Y.-Y. Abscisic acid plays an important role in the regulation of strawberry fruit ripening. *Plant Physiol.* **2011**, *157*, 188–199. https://doi.org/10.1104/pp.111.177311
13. Given, N.K.; Venis, M. A.; Gierson, D. Hormonal regulation of ripening in the strawberry, a non-climacteric fruit. *Planta* **1988**, *174*, 402–406. https://doi.org/10.1007/BF00959527
14. Gu, T.; Jia, S.; Huang, X.; Wang, L.; Fu, W.; Huo, G.; Gan, L.; Ding, J.; Li, Y. Transcriptome and hormone analyses provide insights into hormonal regulation in strawberry ripening. *Planta* **2019**, *250*, 145–162. https://doi.org/10.1007/s00425-019-03155-w
15. Chen, K.; Li, G.-J.; Bressan, R.A.; Song, C.-P.; Zhu, J.-K.; Zhao, Y. Abscisic acid dynamics, signaling, and functions in plants. *J. Integr. Plant Biol.* **2020**, *62*, 25–54. https://doi.org/10.1111/jipb.12899
16. Rai, M.K.; Shekhawat, N.S.; Harish, Gupta, A.K.; Phulwaria, M.; Ram, K.; Jaiswal, U. The role of abscisic acid in plant tissue culture: A review of recent progress. *Plant Cell Tissue Organ Cult.* **2011**, *106*, 179–190. https://doi.org/10.1007/s11240-011-9923-9
17. Finkelstein, R. Abscisic acid synthesis and response. *The Arabidopsis Book/American Society of Plant Biologists* **2013**, *11*, e0166. https://doi.org/10.1199/tab.0166
18. Kushiro, T.; Okamoto, M.; Nakabayashi, K.; Yamagishi, K.; Kitamura, S.; Asami, T.; Hirai, N.; Koshiba, T.; Kamiya, Y.; Nambara, E. The Arabidopsis cytochrome P450 CYP707A encodes ABA 8′-hydroxylases: Key enzymes in ABA catabolism. *EMBO J.* **2004**, *23*, 1647–1656. https://doi.org/10.1038/sj.emboj.7600121
19. Lim, E.-K.; Doucet, C. J.; Hou, B.; Jackson, R.G.; Abrams, S.R.; Bowles, D.J. Resolution of (+)-abscisic acid using an Arabidopsis glycosyltransferase. *Tetrahedron: Asymmetry* **2005**, *16*, 143–147. https://doi.org/10.1016/j.tetasy.2004.11.062
20. Liu, Z.; Yan, J.-P.; Li, D.-K.; Luo, Q.; Yan, Q.; Liu, Z.-B.; Ye, L.-M., Wang, J.-M.; Li, X.-F.; Yang, Y. UDP-Glucosyltransferase71C5, a major glucosyltransferase, mediates abscisic acid homeostasis in Arabidopsis. *Plant Physiol.* **2015**, *167*, 1659–1670. https://doi.org/10.1104/pp.15.00053
21. Lee, K. H.; Piao, H. L.; Kim, H.-Y.; Choi, S. M.; Jiang, F.; Hartung, W.; Hwang, I.; Kwak, J. M.; Lee, I.-J.; Hwang, I. Activation of glucosidase via stress-induced polymerization rapidly increases active pools of abscisic acid. *Cell* **2006**, *126*, 1109–1120. https://doi.org/10.1016/j.cell.2006.07.034
22. Bai, Q.; Huang, Y.; Shen, Y. The physiological and molecular mechanism of abscisic acid in regulation of fleshy fruit ripening. *Front. Plant Sci.* **2021**, *11*. https://doi.org/10.3389/fpls.2020.619953
23. Cutler, S.R.; Rodriguez, P.L.; Finkelstein, R.R.; Abrams, S.R. Abscisic acid: Emergence of a core signaling network. *Annu. Rev. Plant Biol.* **2010,** *61*, 651–679. https://doi.org/10.1146/annurev-arplant-042809-112122
24. Hao, Q.; Yin, P.; Li, W.; Wang, L.; Yan, C.; Lin, Z.; Wu, J. Z.; Wang, J.; Yan, S. F.; Yan, N. The molecular basis of ABA-independent inhibition of PP2Cs by a subclass of PYL proteins. *Mol. Cell* **2011**, *42*, 662–672. https://doi.org/10.1016/j.molcel.2011.05.011
25. Ji, K.; Chen, P.; Sun, L.; Wang, Y.; Dai, S.; Li, Q.; Li, P.; Sun, Y.; Wu, Y.; Duan, C.; Leng, P.; Ji, K.; Chen, P.; Sun, L.; Wang, Y.; Dai, S.; Li, Q.; Li, P.; Sun, Y.; et al. Non-climacteric ripening in strawberry fruit is linked to ABA, FaNCED2 and FaCYP707A1. *Funct. Plant Biol.* **2012**, *39*, 351–357. https://doi.org/10.1071/FP11293
26. Hou, B.-Z.; Chen, X.-H.; Shen, Y.-Y. Interactions between strawberry ABA receptor PYR/PYLs and protein phosphatase PP2Cs on basis of transcriptome and yeast two-hybrid analyses. *J. Plant Growth Regul.* **2021**, *40*, 594–602. https://doi.org/10.1007/s00344-020-10121-4
27. Liao, X.; Li, M.; Liu, B.; Yan, M.; Yu, X.; Zi, H.; Liu, R.; Yamamuro, C. Interlinked regulatory loops of ABA catabolism and biosynthesis coordinate fruit growth and ripening in woodland strawberry. *Proc. Natl. Acad. Sci. USA* **2018**, *115*, E11542–E11550. https://doi.org/10.1073/pnas.1812575115
28. Opazo, M.C.; Lizana, R.; Pimentel, P.; Herrera, R.; Moya-León, M.A. Changes in the mRNA abundance of FcXTH1 and FcXTH2 promoted by hormonal treatments of *Fragaria chiloensis* fruit. *Postharvest Biol. Technol.* **2013**, *77*, 28–34. https://doi.org/10.1016/j.postharvbio.2012.11.007
29. Carrasco-Orellana, C.; Stappung, Y.; Mendez-Yañez, A.; Allan, A.C.; Espley, R.V.; Plunkett, B.J.; Moya-Leon, M.A.; Herrera, R. Characterization of a ripening-related transcription factor FcNAC1 from *Fragaria chiloensis* fruit. *Sci. Rep.* **2018**, *8*, 10524. https://doi.org/10.1038/s41598-018-28226-y

30. Méndez-Yañez, A.; González, M.; Carrasco-Orellana, C.; Herrera, R.; Moya-León, M.A. Isolation of a rhamnogalacturonan lyase expressed during ripening of the Chilean strawberry fruit and its biochemical characterization. *Plant Physiol. Biochem.* **2020**, *146*, 411–419. https://doi.org/10.1016/j.plaphy.2019.11.041
31. Messing, S.A.J.; Gabelli, S.B.; Echeverria, I.; Vogel, J.T.; Guan, J.C.; Tan, B.C.; Klee, H.J.; McCarty, D.R.; Amzel, L.M. Structural insights into maize *Viviparous14*, a key enzyme in the biosynthesis of the phytohormone abscisic Acid. *Plant Cell* **2010**, *22*, 2970–2980. https://doi.org/10.1105/tpc.110.074815
32. Ruiz-Partida, R.; Rosario, S.M.; Lozano-Juste, J. An update on crop ABA receptors. *Plants* **2021**, *10*, 1087. https://doi.org/10.3390/plants10061087.
33. Melcher, K.; Ng, L.-M.; Zhou, X.E.; Soon, F.-F.; Xu, Y.; Suino-Powell, K. M.; Park, S.-Y.; Weiner, J.J.; Fujii, H.; Chinnusamy, V.; Kovach, A.; Li, J.; Wang, Y.; Li, J.; Peterson, F.C.; Jensen, D.R.; Yong, E.-L.; Volkman, B.F.; Cutler, S. R.; … Xu, H. E. A gate-latch-lock mechanism for hormone signaling by abscisic acid receptors. *Nature* **2009**, *462*, 602–608. https://doi.org/10.1038/nature08613
34. Yin, P.; Fan, H.; Hao, Q.; Yuan, X.; Wu, D.; Pang, Y.; Yan, C.; Li, W.; Wang, J.; Yan, N. Structural insights into the mechanism of abscisic acid signaling by PYL proteins. *Nat. Struct. Mol. Biol.* **2009**, *16*, 1230–1236. https://doi.org/10.1038/nsmb.1730
35. Cheng, D.; Wang, Z.; Li, S.; Zhao, J.; Wei, C.; Zhang, Y. Genome-wide identification of CCD gene family in six Cucurbitaceae species and its expression profiles in melon. *Genes* **2022**, *13*, 262. https://doi.org/10.3390/genes13020262
36. Yue, X.-Q.; Zhang, Y.; Yang, C.-K.; Li, J.-G.; Rui, X.; Ding, F.; Hu, F.-C.; Wang, X.-H.; Ma, W.-Q.; Zhou, K.-B. Genome-wide identification and expression analysis of carotenoid cleavage oxygenase genes in Litchi (*Litchi chinensis* Sonn.) *BMC Plant Biology* **2022**, *22*, 394. https://doi.org/10.1186/s12870-022-03772-w
37. Gaete-Eastman, C.; Stappung, Y.; Molinett, S.; Urbina, D.; Moya-León, M.A.; Herrera, R. RNAseq, transcriptome analysis and identification of DEGs involved in development and ripening of *Fragaria chiloensis* fruit. *Front. Plant Sci.* **2022**, 13, 976901. https://doi: 10.3389/fpls.2022.976901
38. Wei, Y.; Wan, H.; Wu, Z.; Wang, R.; Ruan, M.; Ye, Q.; Li, Z.; Zhou, G.; Yao, Z.; Yang, Y. A comprehensive analysis of carotenoid cleavage dioxygenases genes in *Solanum lycopersicum*. *Plant Mol. Biol. Rep*. **2016**, *34*, 512–523. https://doi.org/10.1007/s11105-015-0943-1.
39. Walter, M.H.; Strack, D. Carotenoids and their cleavage products: Biosynthesis and functions. *Nat. Prod Rep.* **2011**, *28*, 663–692. https://doi.org/10.1039/c0np00036a.
40. Sun, Z.; Hans, J.; Walter, M.H.; Matusova, R.; Beekwilder, J.; Verstappen, F.W.A. et al. Cloning and characterisation of a maize carotenoid cleavage dioxygenase (ZmCCD1) and its involvement in the biosynthesis of apocarotenoids with various roles in mutualistic and parasitic interactions. *Planta* **2008**, *228*, 789–801. https://doi.org/10.1007/s00425-008-0781-6.46.
41. Ilg A, Beyer P, Al-Babili S. Characterization of the rice carotenoid cleavage dioxygenase 1 reveals a novel route for geranial biosynthesis. *FEBS J.* **2009**, *276*, 736–747. https://doi.org/10.1111/j.1742-4658.2008.06820.x
42. Ohmiya, A.; Kishimoto, S.; Aida, R.; Yoshioka, S.; Sumitomo, K. Carotenoid cleavage dioxygenase (CmCCD4a) contributes to white color formation in chrysanthemum petals. *Plant Physiol.* **2006**, *142*, 1193–1201. https://doi.org/10.1104/pp.106.087130
43. García-Limones, C.; Schnäbele, K.; Blanco-Portales, R.; Luz Bellido, M.; Caballero, J.L.; Schwab, W.; Muñoz-Blanco, J. Functional characterization of FaCCD1: A carotenoid cleavage dioxygenase from strawberry involved in lutein degradation during fruit ripening. *J. Agric. Food Chem*. **2008**, *56*, 9277–9285.
44. Floss, D.S.; Walter, M.H. Role of carotenoid cleavage dioxygenase 1 (CCD1) in apocarotenoid biogenesis revisited. *Plant Signaling Behav.* **2009**, 4, 172–175.
45. Adami, M.; De Franceschi, P.; Brandi, F.; Liverani, A.; Giovannini, D.; Rosati, C.; Dondini, L.; Tartarini, S. Identifying a carotenoid cleavage dioxygenase (CCD4) gene controlling yellow/white fruit flesh color of peach. *Plant Mol. Biol. Rep*. **2013**, *31*, 1166–1175. https://doi.org/10.1007/s11105-020-01213-2
46. Rodrigo, M.J.; Alquézar, B.; Alós, E.; Medina, V.; Carmona, L.; Bruno, M.; Al-Babili, S.; Zacarías, L. A novel carotenoid cleavage activity involved in the biosynthesis of Citrus fruit-specific apocarotenoid pigments. *J. Exp. Bot.* **2013**, *64*, 4461–4478. https://doi.org/10.1093/jxb/ert260.
47. Watanabe, K.; Oda-Yamamizo, C.; Sage-Ono, K.; Ohmiya, A.; Ono, M. Alteration of flower colour in Ipomoea nil through CRISPR/Cas9-mediated mutagenesis of carotenoid cleavage dioxygenase 4. *Transgenic Res.* **2018**, 27, 25–38. https://doi.org/10.1007/s11248-017-0051-0.
48. Zheng, X.; Zhu, K.; Sun, Q.; Zhang, W.; Wang, X.; Cao, H., et al. Natural variation in CCD4 promoter underpins species-specific evolution of red coloration in citrus peel. *Mol. Plant.* **2019**, *12*, 1294–307. https://doi.org/10.1016/j.molp.2019.04.014
49. Wang, R.K.; Wang, C.E.; Fei, Y.Y.; Gai, J.Y.; Zhao, T.J. Genome-wide identification and transcription analysis of soybean carotenoid oxygenase genes during abiotic stress treatments. *Mol. Biol. Rep*. **2013,** 40, 4737–4745. https://doi.org/10.1007/s11033-013-2570-y.

50. Pasare, S.A.; Ducreux, L.J.M.; Morris, W.L.; Campbell, R.; Sharma, S.K.; Roumeliotis, E., et al. The role of the potato (*Solanum tuberosum*) CCD8 gene in stolon and tuber development. *New Phytol.* **2013**, *198*, 1108–1120. https://doi.org/10.1111/nph.12217.
51. Ha, C.V.; Leyva-González, M.A.; Osakabe, Y.; Tran, U.T.; Nishiyama, R.; Watanabe, Y. et al. Positive regulatory role of strigolactone in plant responses to drought and salt stress. *Proc. Natl. Acad. Sci. USA* **2014**, *111*, 851–856. https://doi.org/10.1073/pnas.1322135111.
52. Pan, X.; Zheng, H.; Zhao, J.; Xu, Y.; Li, X. ZmCCD7/ZpCCD7 encodes a carotenoid cleavage dioxygenase mediating shoot branching. *Planta* **2016**, *243*, 1407–1418. https://doi.org/10.1007/s00425-016-2479-5
53. Wheeler, S.; Loveys, B.; Ford, C.; Davies, C. The relationship between the expression of abscisic acid biosynthesis genes, accumulation of abscisic acid and the promotion of *Vitis vinifera* L. berry ripening by abscisic acid. *Aust. J. Grape Wine Res.* **2010**, *15*, 195–204. https://doi.org/10.1111/j.1755-0238.2008.00045.x
54. Shen, X.; Zhou, K.; Liu, L.; Zhang, K.; Yuan, H.; Liao, X.; et al. A role for PacMYBA in ABA-regulated anthocyanin biosynthesis in red-colored sweet cherry cv. Hong Deng (*Prunus avium* L.). *Plant Cell Physiol.* **2014**, 55, 862–880. https://doi.org/10.1093/pcp/pcu013
55. Singh, S.P.; Saini, M.K.; Singh, J.; Pongener, A.; Sidhu, G.S. Preharvest application of abscisic acid promotes anthocyanins accumulation in pericarp of litchi fruit without adversely affecting postharvest quality. *Postharvest Biol. Technol.* **2014**, *96*, 14–22. https://doi.org/10.1016/j.postharvbio.2014.05.005
56. Tian, X.; Ji, J.; Wang, G.; Jin, C.; Guan, C.; Wu, D.; Li, Z. Cloning and expression analysis of 9-cis-epoxycarotenoid dioxygenase gene 1 involved in fruit maturation and abiotic stress response in *Lycium chinense*. *J. Plant Growth Regul.* **2015**, *34*, 465–474. https://doi.org/10.1007/s00344-015-9481-1
57. Zhang, M.; Leng, P.; Zhang, G.; Li, X. Cloning and functional analysis of 9-cis-epoxycarotenoid dioxygenase (NCED) genes encoding a key enzyme during abscisic acid biosynthesis from peach and grape fruits. *J. Plant Physiol.* **2009**, *166*, 1241–1252. https://doi.org/10.1016/j.jplph.2009.01.013
58. Agustí, J.; Zapater, M.; Iglesias, D.J.; Cercós, M.; Tadeo, F.R.; Talón, M. Differential expression of putative 9-cis-epoxycarotenoid dioxygenases and abscisic acid accumulation in water stressed vegetative and reproductive tissues of citrus. *Plant Sci.* **2007**, *172*, 85-94. https://doi.org/10.1016/j.plantsci.2006.07.013
59. Ibdah, M.; Azulay, Y.; Portnoy, V.; Wasserman, B.; Bar, E.; Meir, A.; Burger, Y.; Hirschberg, J.; Schaffer, A.A.; Katzir, N.; Tadmor, Y.; Lewinsohn, E. Functional characterization of CmCCD1, a carotenoid cleavage dioxygenase from melon. *Phytochemistry* 2006, *67*, 1579–1589. https://doi.org/10.1016/j.phytochem.2006.02.00959.
60. Santiago, J.; Dupeux, F.; Round, A.; Antoni, R.; Park, S.Y.; Jamin, M.; Cutler, S.R.; Rodriguez, P.L.; Márquez, J.A. The abscisic acid receptor PYR1 in complex with abscisic acid. *Nature* **2009**, *462*, 665–668. https://doi.org/10.1038/nature08591
61. Wang, G.; Qi, K.; Gao, X.; Guo, L.; Cao,P.; Li, Q.; Qiao, X.; Gu, C.; Zhang, S. Genome-wide identification and comparative analysis of the PYL gene family on eight Rosacease species and expression analysis of seeds germination in pear. *BMC Genomics* **2022**, *23*, 233. https://doi.org/10.1186/s12864-022-08556-1
62. Zhao, Y.; Qi, G.; Ren, F.; Wang, Y.; Wang, P.; Wu, X. Analysis of PYL genes and their potential relevance to stress tolerance and berry ripening in grape. *J. Amer. Soc. Hort. Sci.* **2020**, 145, 308–317. https://doi.org/10.21273/JASHS04942-20
63. Romero, P.; Lafuente, M.T.; Rodrigo, M.J. The citrus ABA signalosome: Identification and transcriptional regulation during sweet orange fruit ripening and leaf dehydration. *J. Exp. Bot.* **2012**, *63*, 4931–4945. https://doi.org/10.1093/jxb/ers168
64. Gonzalez-Guzman, M.; Pizzio, G.A.; Antoni, R.; Vera-Sirera, F.; Merilo, E.; Bassel, G.W.; Fernandez, M.A.; Holdsworth, M.J.; Perez-Amador, M.A.; Kollist, H.; et al. Arabidopsis PYR/PYL/RCAR receptors play a major role in quantitative regulation of stomatal aperture and transcriptional response to abscisic acid. *Plant Cell* **2012**, *24*, 2483–2496.
65. Kai, W.; Wang, J.; Liang, B.; Fu, Y.; Zheng, Y.; Zhang, W.; Li, Q.; Leng, P. PYL9 is involved in the regulation of ABA signaling during tomato fruit ripening. *J. Exp. Bot.* **2019**, *70*, 6305–6319. https://doi.org/10.1093/jxb/erz396.
66. Jung, S.; Lee, T.; Cheng, C.-H.; Buble, K.; Zheng, P.; Yu, J.; Humann, J.; Ficklin, S. P.; Gasic, K.; Scott, K.; Frank, M.; Ru, S.; Hough, H.; Evans, K.; Peace, C.; Olmstead, M.; DeVetter, L. W.; McFerson, J.; Coe, M.; … Main, D. 15 years of GDR: New data and functionality in the Genome Database for Rosaceae. *Nucleic Acids Res.* **2019**, *47*, D1137–D1145. https://doi.org/10.1093/nar/gky1000
67. Gaete-Eastman, C.; Mattus-Araya, E.; Herrera, R.; Moya-León, M.A. Evaluation of reference genes for transcript normalization in *Fragaria chiloensis* fruit and vegetative tissues. *Physiol. Mol. Biol. Plants* **2022**, *28*, 1535-1544. https://doi:10.1007/s12298-022-01227-y

 doi:10.20944/preprints202304.0574.v1